WWW.IJRPR.COM

International Journal of Research Publication and Reviews

Journal homepage: www.ijrpr.com ISSN 2582-7421

Optimization of the factors affecting the Photovoltaic Performance of Methylammonium Lead Iodide Perovskite Solar Cell using SCAPS-1D Software

Wumani Victor Zhiya[a, b], Donald Dehiin Hile[a, c], Ilemona Sunday Omeje[d], Martins Ajev [a], Felix Igbasue Ortwer [a], Titus Enemona Ogbe [e]

[a](Department of Industrial Physics, Joseph Sarwuan Tarka University, Makurdi, Formally Known as Federal University of Agriculture, Makurdi, Benue State, Nigeria)
[b](Department of Physics, Federal University of Technology, Minna, Niger State, Nigeria)
[c](Department of Physics, University of Zululand, KwaDlangezwa, 3886, South Africa)
[d](Laboratoire Hubert Curien, UMR CNRS 5516, Universite Jean Monnet, Universite de Lyon, Saint-Etienne, France)
[e](Department of Physics, Kogi State University, Anyigba, Kogi State, Nigeria)
Email: zhiyavic@gmail.com

ABSTRACT

In this work, the factors affecting the photovoltaic performance of methylammonium iodide ($MAPbI_3$) were optimized at different values. The factors investigated Absorber layer thickness, electron transport material (ETM) thickness, hole transport material (HTM) thickness, the electron affinity (EA) of ETM, the EA of HTM, and the band gap of the absorber layer. The results shows that the open circuit voltage (V_{OC}), short circuit current density (J_{SC}) and power conversion efficiency (PCE) increases with the increase in the absorber layer thickness, while the fill factor (FF) decreases with an increase in the absorber layer thickness. Only the V_{OC} increases with the increase in the ETM thickness, while the values of the $J_{SC,}$ FF and PCE decreases with increase in the ETM thickness. The V_{OC}, J_{SC} and PCE were observed to increase with an increase the HTM thickness, while the FF decreases with the increase in the HTM thickness from 0.010 µm – 0.400 µm and then increases with HTM thickness of 0.500 µm 1.000 µm.

The photovoltaic performance varies with increasing values of the EA of the ETM, the V_{OC}, $J_{SC,}$ FF, and PCE increases at some values of the ETM EA, while their values decreases at some other values of the, ETM EA. The V_{OC} and PCE decreases at some values of the EA of the HTM, while increases at some other values of the EA of the HTM. The J_{SC} and FF increases with increase in the EA of the HTM.

The V_{OC}, FF and PCE were observed to decrease at some values of the absorber layer band gap and increase at some other values of the band. The J_{SC} was found to decrease with an increase in the absorber layer band gap.

The simulation with the optimized parameters yielded an improved performance in the PCE with the V_{OC} of 0.69 V, J_{SC} of 43.03 Ma/cm^2, FF of 77.79 % and PCE of 23.07. this study revealed the importance of optimization in the improvement of the photovoltaic performance of the photovoltaic performance of $MAPbI_3$ perovskite solar cells.

Keywords: Thickness, band gap, electron affinity, open circuit voltage, short circuit current density, fill factor and power conversion efficiency.

1 Introduction

The most popular renewable energy source is solar energy has become due to its natural abundant and less harmful environment and living beings. It the means of converting solar radiation into electricity directly through photovoltaic (PV) technology, which has received tremendous acceptance as one of the most leading potentials for sustainable and environmental friendly energy-producing technologies [21]. The major hindrances preventing the generation of power from photovoltaic-based technologies are the low PCE and the high cost of materials [12]. Therefore, researchers in photovoltaic field are coming up with various new concepts of solar-cell architecture and formation that are environmental friendly, cost, stability, and large quantity production. Some of the materials which have potential prospects for PV-based electricity generation includes silicon, copper-indium-gallium-selenide (CIGS) and cadmium telluride [11, 13]. Silicon-based PVs have been mostly controlling the present marketplace (almost 90%) is applicable for industrial applications due to long-term stability and high-power conversion efficiency (PCE) compare to others [23]. High melting point temperature (1400 °C) and needing for expensive instruments for the fabrication of Si solar cells and stagnated power conversion efficiency are the biggest

challenge for the production of low-cost solar cells [10, 19]. Apart from Si, CIGS-based solar cells have also attracted a lot of attention from the scientific community because to their superior characteristics and lower cost compared to typical silicon-based solar cells. Despite the high performance of CIGS solar cells, the PCE of single-junction CIGS solar cells has limited applications as a result of its inability to capture a wider range of the solar insolation.

PSCs have emerge as potential contenders for achieving high performance with minimal fabrication cost due to their suitable optoelectronic properties which includes high absorption coefficient in the visible band [4]. Solar cells have thus far attained an outstanding efficiency of 25.7% [5]. In particularly, the low-price environmental friendly and abundant organic-inorganic halide perovskite photovoltaics started to flourish in 2009 as a result of the rapid increase in its PCE [16, 1]. Different deposition techniques are used for perovskite layer which ranges from spin-coating, deep coating, doctor blade, sequential deposition, vacuum deposition, and spray pyrolysis. Generally, perovskite solar cells are made up of five layers which are the transparent conducting oxide, electron transporting layer, absorber layer, hole transporting layer and the back contact electrode. The function demonstrated by each layer in PSC should be understood in order to enhance the performance of the device [18]. TiO^2 is considered the mostly used ETM for PSCs device due to its high performance in solar cells as a result of its proper band gap, high transmittance, suitable energy level for electron injection, high electron mobility, good stability and environmental friendliness [27]. However, obtaining good quality film of either compact or mesoporous TiO^2 requires high annealing temperature, which limits its application in solar devices and results to increase in the production cost. Consequently, the electron mobility of perovskite materials is ~7.5 $cm^2V^{-1}s^{-1}$ and that of TiO^2 ranged between 0.1– 4.0 $cm^2V^{-1}s^{-1}$. These lower values of electron mobility in TiO^2 may result to shortfall in performance of solar cells [14]. The ETM is used to compensate and balance the difference of hole and electron diffusion lengths [27, 5]. In addition, the ETM is a blocking layer that prevents holes from reaching the fluorine-doped tin oxide or Indium doped tin oxide (FTO or ITO) electrode. For high performance solar cells, ETMs should be selected in such a manner that it possesses good optical transmittance in the visible range to reduce the optical energy loss, a good energy levels matching with that of perovskite materials to improve the electron extraction efficiency and block holes and good electron mobility. As a result, the design and materials properties of the ETM are crucial for solar cell performance [27, 15].

Methyl ammonium lead iodide ($CH_3NH_3PbI_3$) with a band gap of 1.50 *eV* that covers absorption within wide range of visible spectrum was reported by various experimental and

theoretical studies[15, 22]. Lead based perovskites materials are considered as promising candidates for future-generation photovoltaics owing to their unique optoelectronic properties and very low fabrication cost.[7].

The most commonly used hole transport material is Spiro- OMeTAD which is organic in nature [25].

2 Device Structure and Simulation Methodology

2.1 Device Structure and Modeling

In this research, a one-dimensional planar n-i-p perovskite device (FTO/ZnO_2/$MAPbI_3$/CuO/Au) (Figure 1a) was simulated using the Solar Cell Capacitance Simulator (SCAPS-1D) software.

The simulation, which is based on a classical drift-diffusion model, is carried out at 300-K under one sun (AM1.5G, 100 mW cm^{-2}) irradiation [15]. $MAPbI_3$ (1.50eV) was used as the absorber layer, which is sandwiched between Zinc oxide ETL and Cupper oxide HTL. Figure 1b shows the energy band diagram depicting the flow of charge carriers in the device constituting $MAPbI_3$ perovskites along with the ETL, HTL and contacts.

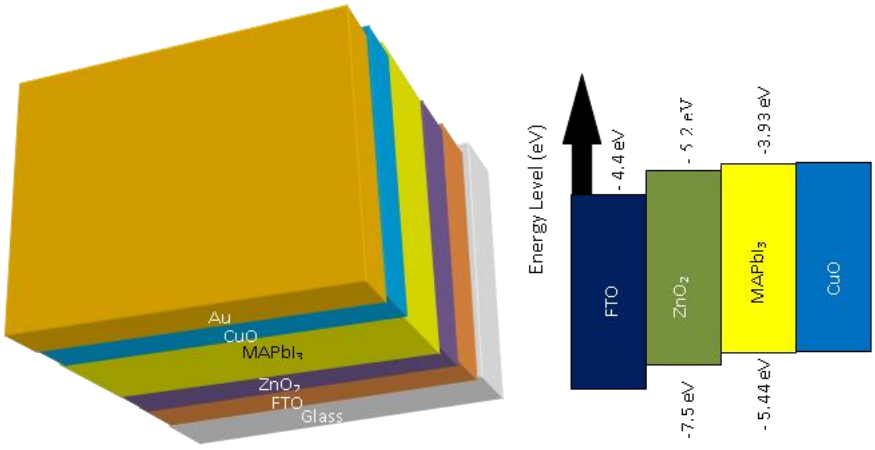

a) **(b)**

Figure 1: (a) Schematic structure of the simulated PSCs, (b) Energy Band Alignment of the used materials.

2.2 Simulation Methodology

Device simulation is a strong tool to understand device physics and optimum design for efficiency improvement. In particular, Solar Cell Capacitance Simulator 1-dimensional (SCAPS-1*D*) is a simulation program that calculates energy bands, concentrations and currents, *J–V* characteristics and spectral response among other device parameters by solving the three basic semiconductor equations under the constraint of boundary conditions. SCAPS-1D simulations are mainly based on three basic equations namely the Poisson's equation, electron continuity equation and hole continuity equation respectively. It is a one dimensional solar cell simulation program that was developed at the department of Electronics and Information Systems (ELIS) of the University of Gent, Belgium [3]. The software is designed to perform up to a maximum of seven semiconductor layers and along with this, it provides the flexibility of grading and tuning different properties such as bandgap, electron affinity, defects, doping, interfacial properties etc. for each of the layers. The spectral condition under which the simulation was performed is AM 1.5G 1 sun spectrum. The properties of each of ETL, HTL and the absorber layer of Methylammonium Lead Iodide ($MAPbI_3$) perovskite layers were varied in the optimisation. The thickness, band gap and doping concentration were varied within a feasible range in order to study the effects changing values on the current-voltage characteristics of the device. The following equations play significant roles in the simulation. Poisson's Equation for a semiconductor is represented in equation 1. [24].

$$\frac{d2\psi(x)}{dx2} = \frac{q}{\varepsilon}(n - p + NA - ND) \quad (1)$$

Where, ε is the permittivity of the semiconductor, NA represents the acceptor concentration,

ND is the donor concentration and ψ resembles the electrostatic potential.

Now, the electron and hole continuity equations for a semiconductor are given by:

Electron continuity equation is presented in equation 2. [24].

$$\frac{\partial Jn(x)}{\partial x} - q\frac{\partial n}{\partial t} = + qR \quad (2)$$

Hole continuity equation is presented in equation 3. [24].

$$\frac{\partial Jp(x)}{\partial x} + q\frac{\partial p}{\partial t} = - qR \quad (3)$$

In the above equations (2) and (3), Jn is the current density for electrons, JP is symbolic of the

current density for holes and R represents the rate of carrier recombination.

Another very important set of equations is the Drift-Diffusion current relations that are given

by the continuity equations shown in (4) and (5). Current is conductor in a semiconductor in two ways through diffusion current and the drift current that is build up due to the drift of minority charge carriers under the influence of electric field.

$$Jn = qn\mu nE + qDn\frac{\partial n}{\partial x} \quad (4)$$

$$Jp = qp\mu pE - qDp\frac{\partial p}{\partial x} \quad (5)$$

Where, Dp is the diffusion coefficient for holes and Dn is the electrons diffusion coefficient.

E represents the electric field, q is the quantity of charge, n and p represents the number of electrons and holes. μn and μp represents the mobility of electron and holes. Other relations that govern the performance parameters are as follows: For open circuit voltage:

$$V_{OC} = \frac{nkT}{q} = \ln\left(\frac{JSC}{JS} + 1\right) \quad (6)$$

Where, J_{SC} is the short circuit current density (or, light generated current), J_S is the reverse

saturation current.

For short circuit current density:

$$J_{SC} = - JL \quad (7)$$

Fill factor and efficiency is given by the relation:

$$FF = \frac{Pmax}{JSC\ VOC} \quad (8)$$

$$\eta\ (PCE) = \frac{Pmax}{Pin} = \frac{FF \times JSC \times VOC}{Pin} \quad (9)$$

For better device performance, the electron transport layer, light absorbing layer of solar cell and the hole transport layer plays significant roles. In this simulation the thickness and band gap of the electron transport layer, absorber layer and hole transport layer of $MAPbI_3$ perovskite materials was optimize to achieve higher performances. The layer parameters that were used for this simulation process are presented in Table 1. Some values were derived from existing literatures, while the others were been optimized.

Table1: physical properties for various layers of $MAPbI_3$ perovskite device used for the simulation.

The most useful cell parameters required for the simulation were shown in Table 1. These values were chosen on the basis of theoretical considerations, experimental data and existing literature or in some cases, reasonable estimates. The parameters were estimated, the most important parameters (bandgap (Eg), electron mobility (μ_n), hole mobility (μ_n) etc.) for the simulation were obtained from review of literature. The work function of the cathode electrode (Au) is 5.1 eV which serves as back metal contact.

Table 1: Simulation parameters

Characteristics	**FTO**	**ZnO_2**	**$MAPbI_3$**	**CuO**
Thickness (*μm*)	0.050	0.030	0.500	0.300
Bandgap (eV)	3.500	3.200[26]	1.50	1.3[2]
Electron affinity (eV)	4.200	4.2[Wei, 2018]	4.500	4.500
Dielectric permittivity(relative)	10.000	10.000	10.000	10.000
CB effective density of state (1/cm^3)	1.000E+19	1.000E+19	1.000E+19	1.000E+19
VB effective density of state (1/cm^3)	1.000E+19	1.000E+19	1.000E+19	1.000E+19
Electron thermal velocity (cm/s)	1.000E+7	1.000E+7	1.000E+7	1.000E+7
Hole thermal velocity (cm/s)	1.000E+7	1.000E+7	1.000E+7	1.000E+7
Electron mobility (cm/s)	5.000E+1	5.000E+1	5.000E+1	5.000E+1
Hole mobility (cm/s)	5.000E+1	5.000E+1	5.000E+1	5.000E+1
Effective mass of electron	1.000E+0	1.000E+0	1.000E+0	1.000E+0
Effective mass of hole	1.000E+0	1.000E+0	1.000E+0	1.000E+0
Shallow uniform donor density ND ($1/cm^3$)	1.000E+17	1.000E+15	0	0
Shallow uniform acceptor density NA ($1/cm^3$)	0	0	1.000E+13	1.000E+15
Defect type	Neutral	Neutral	Neutral	Neutral
Gold back contact with 5.1 eV workfuction				

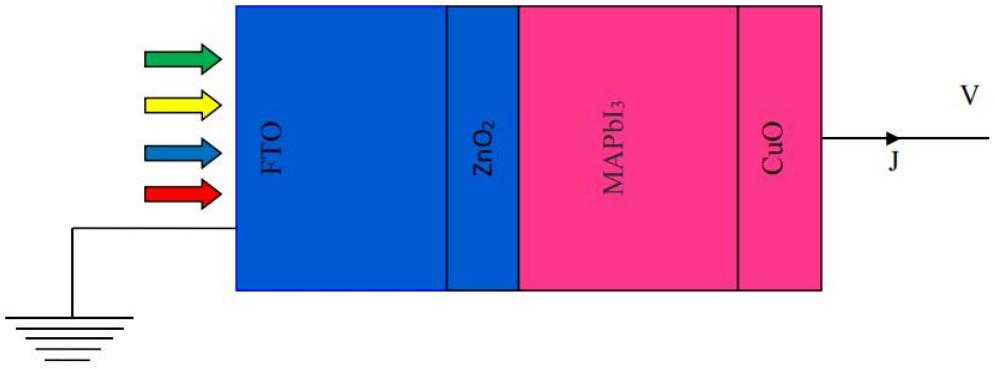

Figure 2: Perovskite Simulation Structure

The J-V characteristic curve obtained by simulating with the data in Table 1 is shown in Figure 3 with the output cell parameters V_{OC} = 0.7510V, J_{SC} = 30.739246 mA/ cm^2, FF = 46.26%, and PCE = 10.68% under AM1.5 simulated sunlight of 1000W/ cm^2 at 300K.

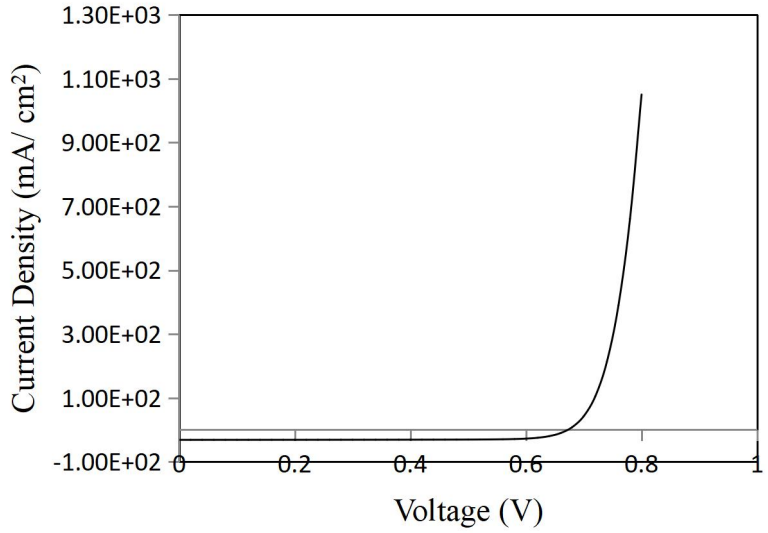

Figure 3: J–V curve of PSC with initial parameters

3 Resuls and Discussions

3.1 Effect of Absorber Thickness on Device Performance

The values of the device performance were presented in Table 2. The influence of thickness of absorber with variation of performance parameters is shown in the Figure 4.The impact of the absorber layer was study by varying the layer thickness from 0.010 – 1.000 µm. It was found that there is a steady increase in the open circuit voltage (V_{OC}), short circuit current (J_{SC}) and power conversion efficiency (PCE) with increase in the absorber layer thickness (Figure 4a, b and d) [20, 9]. The fill factor (FF) decreases with an increase in the absorber layer thickness, but it increases at certain values of the thickness (Figure 4c). The increase in J_{SC} is associated with the increase in carrier generation and dissociation, the PCE increase with increase in layer thickness due to the production of new charge carriers [6].

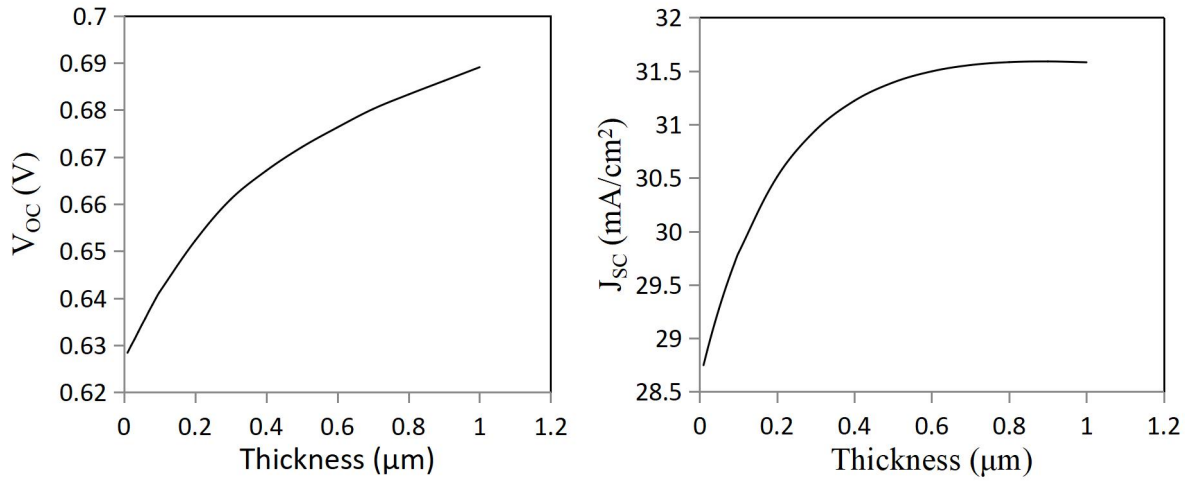

(a) (b)

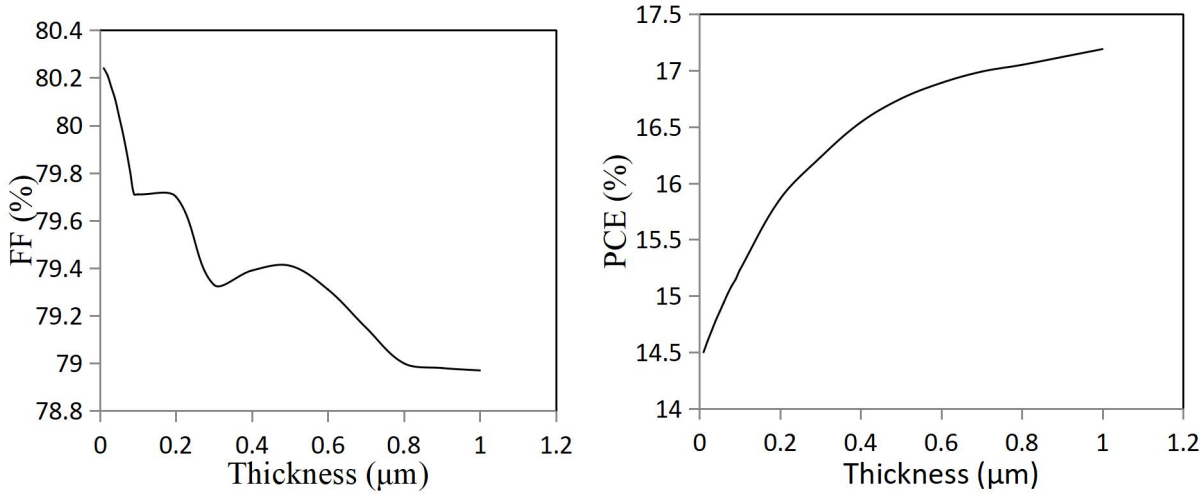

(c) (d)

Figure 4: Photovoltaic Performance vs Absorber Layer Thickness. (a) V_{OC} (V) against Thickness (µm), (b) J_{SC} (mA/cm^2) against Thickness (µm), (c) FF (%) against Thickness (µm) and (d) PCE (%) against Thickness (µm).

Table 2: Values of V_{OC} (V), J_{SC} (mA/cm^2), FF (%) and PCE (%) deduced from the simulation results at various values of Absorber Layer Thickness.

Thickness (µm)	**V_{OC} (V)**	**J_{SC} (mA/cm^2)**	**FF (%)**	**PCE (%)**
0.010	0.6284	28.748642	80.24	14.50
0.020	0.6299	28.891325	80.21	14.60
0.030	0.6313	29.026495	80.16	14.69
0.040	0.6328	29.154520	80.11	14.78
0.050	0.6343	29.275819	80.04	14.86
0.060	0.6357	29.390887	79.97	14.94
0.070	0.6372	29.500080	79.89	15.02
0.080	0.6386	29.603513	79.80	15.09
0.090	0.6400	29.701723	79.71	15.15
0.100	0.6413	29.794987	79.71	15.23
0.200	0.6522	30.509151	79.70	15.86
0.300	0.6610	30.947398	79.33	16.23
0.400	0.6671	31.221591	79.39	16.54
0.500	0.6721	31.392650	79.41	16.75
0.600	0.6763	31.496761	79.31	16.89
0.700	0.6802	31.555687	79.15	16.99
0.800	0.6833	31.583067	79.00	17.05
0.900	0.6862	31.589720	78.98	17.12
1.000	0.6891	31.581629	78.97	17.19

3.2 Effect of Electron Transport Material (ETM) Thickness on Device Performance

The plot of solar cell parameters; V_{OC}, J_{SC}, FF and PCE versus thickness of the ETM is shown in Figure 5. It was revealed that the Voc increases with increase in the ETM thickness, The Jsc and FF and PCE decrease slightly with the increase in the thickness of ETM (Figure 5a, b, c and d). The

decrease in the photovoltaic properties is due to fractional absorption of incident light by the ETM and the surface recombination at the interface which result to lesser electron and hole pairs extraction [6, 8]. The decrease in FF shown in Table 3 is connected to the increase in series resistance [6].

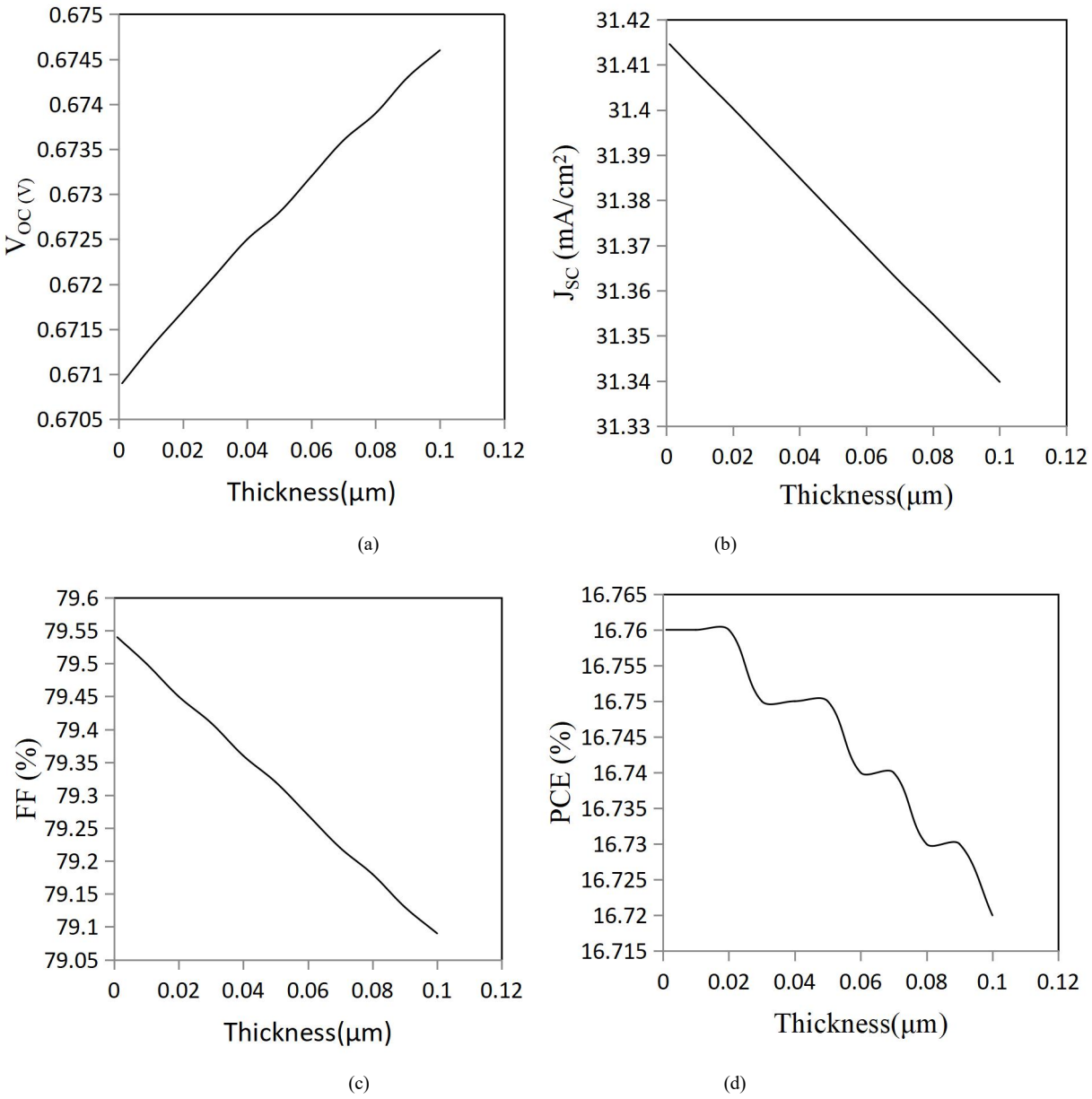

Figure 5: Photovoltaic Performance vs ELT Thickness. (a) V_{OC} (V) against Thickness (μm), (b) J_{SC} (mA/cm^2) against Thickness (μm), (c) FF (%) against Thickness (μm) and (d) PCE (%) against Thickness (μm).

Table 3: Values of V_{OC} (V), J_{SC} (mA/cm^2), FF (%) and PCE (%) deduced from the simulation results at various values of ETL Thickness.

Thickness(μm)	**V_{OC} (V)**	**J_{SC} (mA/cm^2)**	**FF (%)**	**PCE (%)**
0.001	0.6709	31.414544	79.54	16.76
0.010	0.6713	31.407701	79.50	16.76
0.020	0.6717	31.400328	79.45	16.76
0.030	0.6721	31.392650	79.41	16.75
0.040	0.6725	31.384967	79.36	16.75
0.050	0.6728	31.377292	79.32	16.75
0.060	0.6732	31.369638	79.27	16.74

0.070	0.6736	31.362017	79.22	16.74
0.080	0.6739	31.354785	79.18	16.73
0.090	0.6743	31.347288	79.13	16.73
0.100	0.6746	31.339823	79.09	16.72

3.3 Effect of Hole Transport Material (HTM) Thickness on Device Performance

The thickness of the hole transport material was varied from 0.010 - 1.000 µm to study its effects on the photovoltaic parameters of the simulated perovskite solar cell. The thickness of the HTM has a significant impact on the device performance as presented in Table 4. It was observed that the Voc, Jsc, and PCE increase steadily with the increase in the thickness of HTM (Figure 6a, b and d). The FF decreases with increase in HTM Thickness from 0.010 - 0.200 µm and increases when the thickness of the HTM was increased from 0.300 - 1.000 µm (Figure 6c).

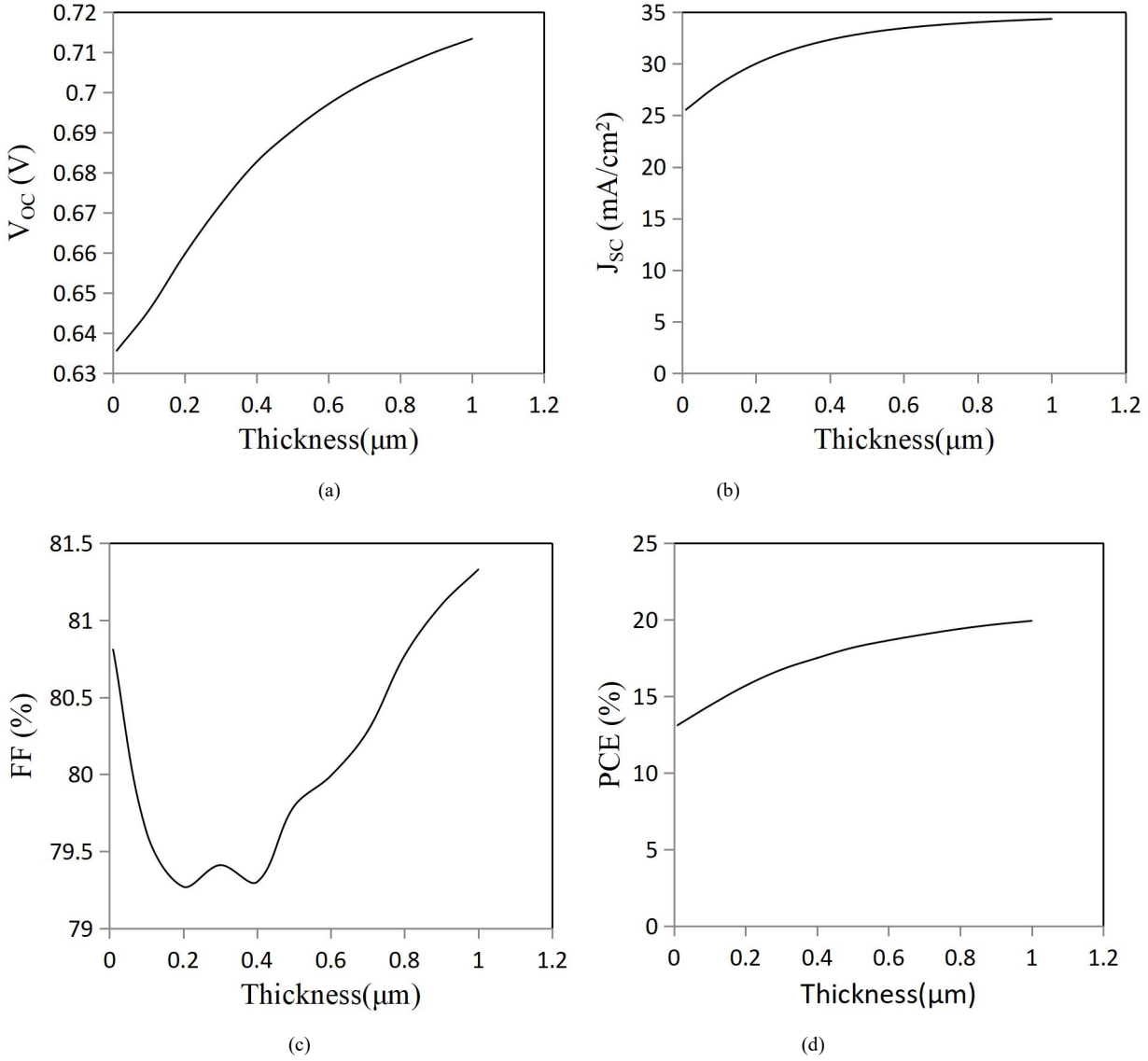

Figure 6: Photovoltaic Performance vs HTM Thickness. (a) V_{OC} (V) against Thickness (µm), (b) J_{SC} (mA/cm^2) against Thickness (µm), (c) FF (%) against Thickness (µm) and (d) PCE (%) against Thickness (µm).

Table 4: Values of V_{OC} (V), J_{SC} (mA/cm^2), FF (%) and PCE (%) deduced from the simulation results at various values of HTM Thickness.

Thickness(μm)	V_{OC} (V)	J_{SC} (mA/cm^2)	FF (%)	PCE (%)
0.010	0.6356	25.551454	80.81	13.12
0.100	0.6457	28.012873	79.63	14.40
0.200	0.6597	30.020319	79.27	15.70
0.300	0.6721	31.392650	79.41	16.75
0.400	0.6827	32.343574	79.30	17.51
0.500	0.6905	33.006127	79.79	18.19
0.600	0.6971	33.467994	79.99	18.66
0.700	0.7024	33.793977	80.28	19.06
0.800	0.7065	34.032503	80.77	19.42
0.900	0.7102	34.215820	81.10	19.71
1.000	0.7134	34.361507	81.33	19.94

3.6 Influence of electron affinity of ETM

The effect of electron affinity (EA) on the performance of perovskite solar cell is examined by varying the values of EA in the range of 4.100 eV to 4.600 eV. Figure 7 shows the plot of the variation of V_{OC}, J_{SC}, FF and PCE with EA. It was observed that the V_{OC} decreases from 0.6714 V - 0.6710 V and increases continually with increase in EA (Figure 7a), the J_{SC} increases as the EA increases from 4.100 eV - 4.300 eV and decreases above 4.400 eV (Figure 7b). The FF and increases with increase in EA but decrease with the EA above 4.300 eV (Figure 7c), while the PCE increases with increase in EA and decrease when the EA is higher than 4.400 eV (Figure 7d). The optimum value of PCE was obtained at EA value of 4.500 eV as shown in Table 5. It is now clear that ETM with good EA can reduce quenching losses in PSCs [6].

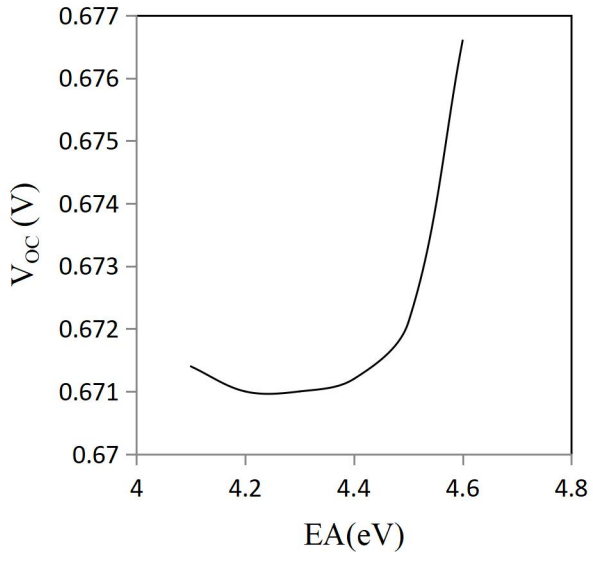

(a)

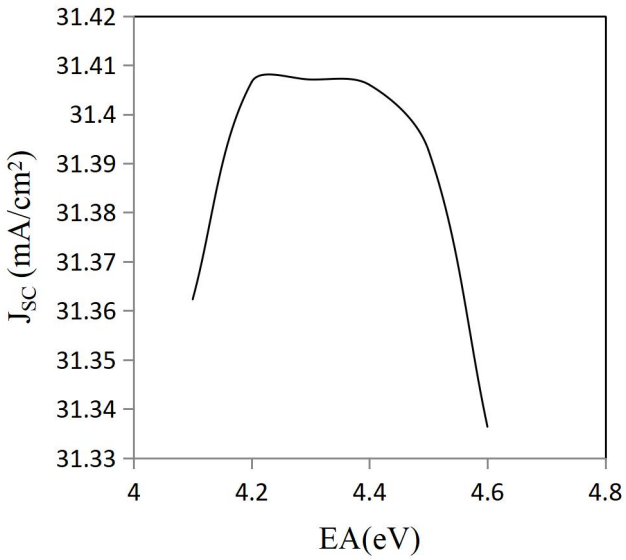

(b)

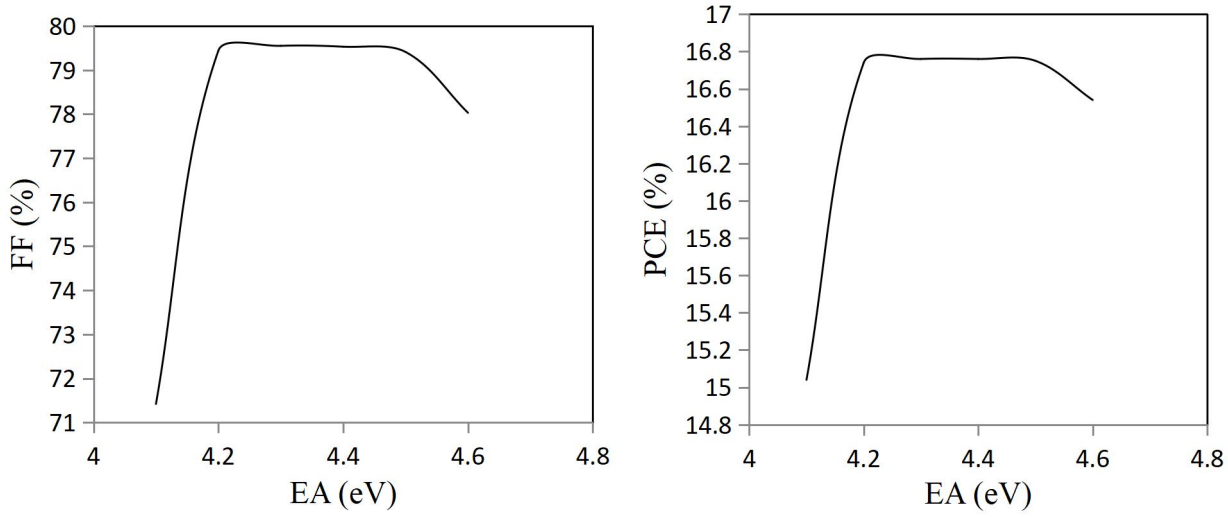

(c) (d)

Figure 7: Photovoltaic Performance vs EA (eV) of the ETM. (a) V_{OC} (V) against EA (eV), (b) J_{SC} (mA/cm^2) against EA (eV), (c) FF (%) against EA (eV and (d) PCE (%) against EA (eV).

Table 5: Values of V_{OC} (V), J_{SC} (mA/cm^2), FF (%) and PCE (%) deduced from the simulation results at various values of electron affinity (EA) (eV) of the ETM.

EA(eV)	V_{OC} (V)	J_{SC} (mA/cm^2)	FF (%)	PCE (%)
4.100	0.6714	31.362302	71.42	15.04
4.200	0.6710	31.406555	79.44	16.74
4.300	0.6710	31.407076	79.55	16.76
4.400	0.6712	31.405984	79.53	16.76
4.500	0.6721	31.392650	79.41	16.75
4.600	0.6766	31.336357	78.03	16.54

3.7 Influence of electron affinity (EA) of HTM.

Figure 8 shows the variation of photovoltaic performance with the EA of the HTM. The V_{OC} decreases continuually with increase in EA (Figure 8a). The J_{SC} and FF were observed to increase continually with increase in EA (Figure 8b and c). The PCE decreases with EA from 4.000 eV - 4.200 eV and increases as the EA increases upto 4.500 eV, it value decrease when the EA was increased to 4.600 eV (Figure 8d). This shows that proper selection of HTM with suitable electron affinity can prevent quenching of carriers and enhanced the performance of PSCs [20, 17]. The values of the photovoltaic performance with respect to increasing HTM EA are presented in Table 6.

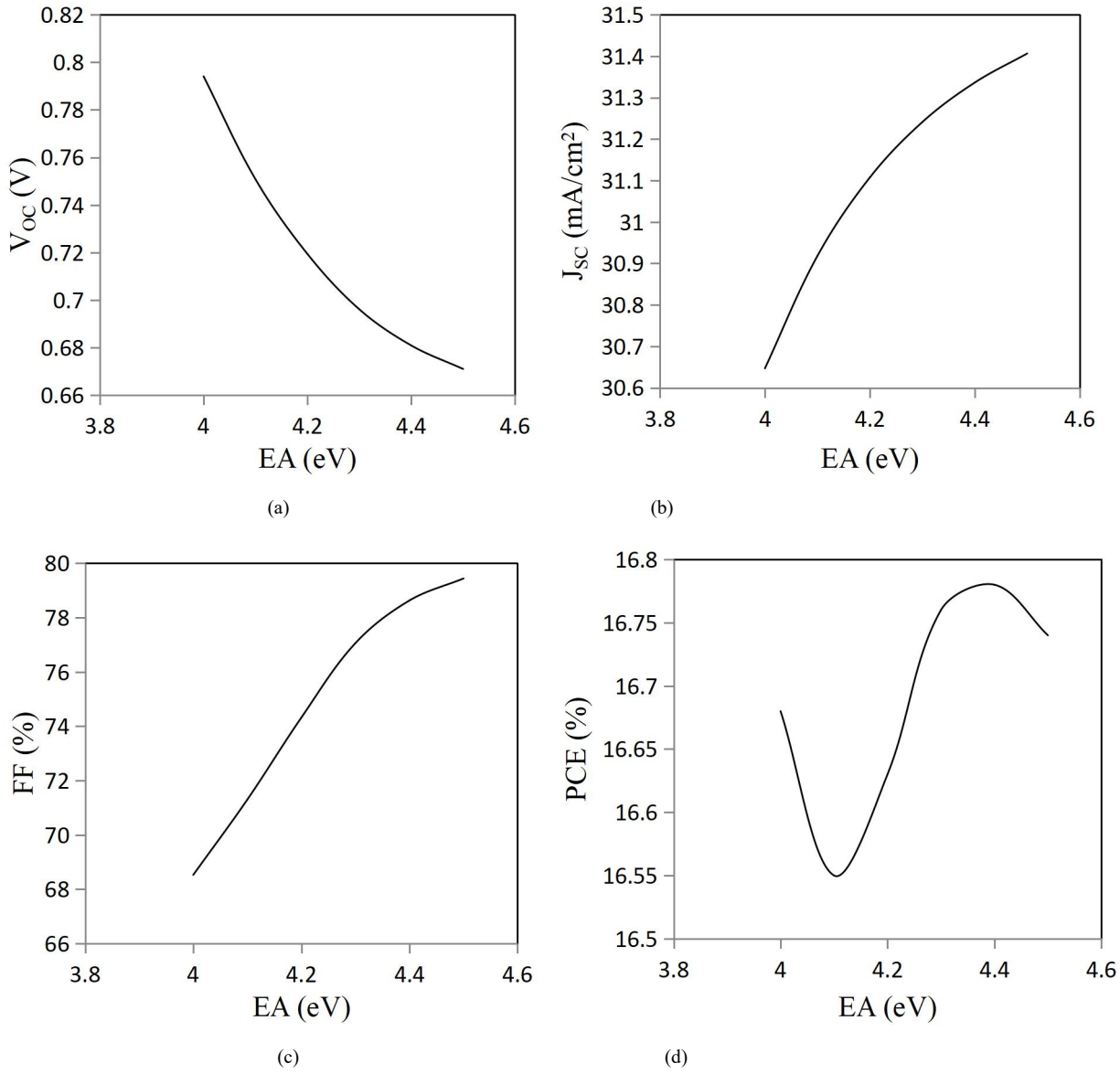

Figure 8: Photovoltaic Performance vs EA (eV) of the HTL. (a)V_{OC} (V) against EA (eV), (b) J_{SC} (mA/cm^2) against EA (eV), (c) FF (%) against EA (eV and (d) PCE (%) against EA (eV).

Table 6: Values of V_{OC} (V), J_{SC} (mA/cm^2), FF (%) and PCE (%) deduced from the simulation results at various values of electron affinity (EA) (eV) of the HTM.

EA(eV)	V_{OC} (V)	J_{SC} (mA/cm^2)	FF (%)	PCE (%)
4.000	0.7941	30.646882	68.53	16.68
4.100	0.7508	30.917987	71.30	16.55
4.200	0.7194	31.107442	74.32	16.63
4.300	0.6961	31.241079	77.06	16.76
4.400	0.6809	31.336421	78.63	16.78
4.500	0.6710	31.406555	79.44	16.74
4.600	0.6800	31.458459	75.53	16.16

3.8 Effect of band gap of absorber layer on the photovoltaic performance

The photovoltaic performance of the simulated PSC varies with the increase in the band gap of the absorber layer. The values photovoltaic parameters obtained with increasing band gap of the absorber layer is presented in Table 7. The V_{OC} increases with increasing band gap from 1.0 eV – 1.3 eV and

decreases as the band gap increases from 1.4 eV – 2.0 eV (Figure 9a). The values of J_{SC}, FF and PCE were observed to be high at lower band gap and decreases continually as the band gap of the absorber layer was increased from 1.1 eV – 2.0 eV as shown in Figure 9b, c and d.

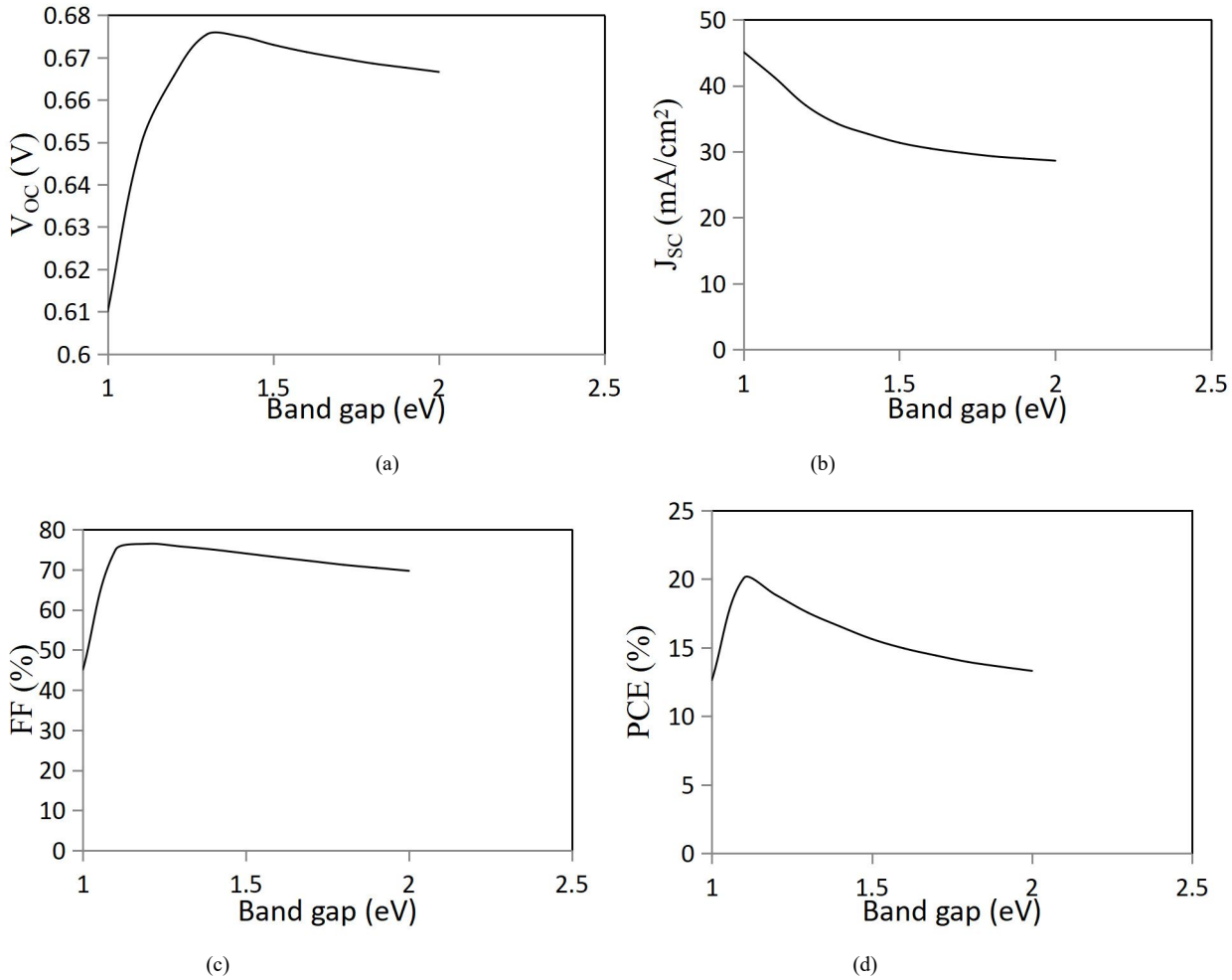

Figure 9: Photovoltaic Performance vs Band gap (eV) of the Absorber Layer. (a)V_{OC} (V) against Band gap (eV), (b) J_{SC} (mA/cm^2) against Band gap (eV), (c) FF (%) against Band gap (eV) and (d) PCE (%) against Band gap (eV).

Table 7: Values of V_{OC} (V), J_{SC} (mA/cm^2), FF (%) and PCE (%) deduced from the simulation results at various values of the band gap of the Absorber layer.

Band gap (eV)	**V_{OC} (V)**	**J_{SC} (mA/cm^2)**	**FF (%)**	**PCE (%)**
1.000	0.6100	45.117956	45.12	12.64
1.100	0.6493	41.239046	74.97	20.07
1.200	0.6657	37.014504	76.44	18.83
1.300	0.6755	34.267149	75.78	17.54
1.400	0.6750	32.674728	75.00	16.54
1.500	0.6730	31.351880	74.03	15.62
1.600	0.6713	30.471104	73.05	14.94
1.700	0.6699	29.836712	72.14	14.42
1.800	0.6686	29.297607	71.20	13.95
1.900	0.6676	28.946614	70.45	13.61
2.000	0.6666	28.634763	69.70	13.30

The simulation with the optimized parameters in Table 8 yielded V_{OC} of 0.69 V, J_{SC} of 43.03 mA/cm^2, FF of 77.79 % and PCE of 23.07 (Figure 10). The high value of PCE is attributed to the increase in the V_{OC} and J_{SC} [20, 6].

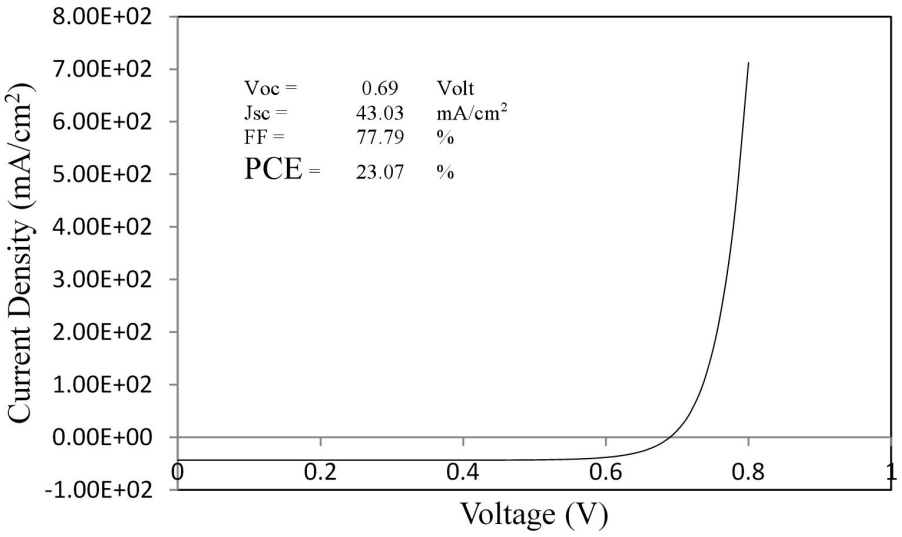

Figure 10: J-V Curve for the optimized paramenters

Table 8: Optimised Simulation parameters

Characteristics	**FTO**	**ZnO_2**	**$MAPbI_3$**	**CuO**
Thickness (µm)	-	0.020	1.000	1.000
Bandgap (eV)	-	-	1.100	-
Electron affinity (eV)	-	4.500	4.300	4.400

Conclusion

The factors affecting the photovoltaic performance of a perovskite solar cell were optimized in this work. The photovoltaic performance of the simulated device with various $MAPbI_3$ thicknesses, ETM thicknesses, HTM, ETM electron affinity, HTM electron affinity and the band gap of $MAPbI_3$ were analyzed. It was observed from the results obtained that the parameters affect the performance of the solar cell. The overall V_{OC}, J_{SC}, , FF, and PCE of 0.6891 V, 43.025994 mA/cm^2, 23. 77.79 %, and 23.07 % respectively were obtained from simulation using the optimised parameters. These results were in agreement with the investigation carried out by 20, and 6.

Funding

This research was funded by the authors without any funding sources from anywhere.

Conflict of Interest

The authors declare that there was no conflict of interest.

Availability of data and materials: The data and materials for this research will be made available on request.

Ethics: Consent to Participate, and Consent to Publish declarations: not applicable.

References

[1] Akkerman, Q. A., Rainò, G., Kovalenko, M. V., & Manna, L. (2018). Genesis, challenges and opportunities for colloidal lead halide perovskite nanocrystals. *Nature materials*, *17*(5), 394-405.

[2) Aktar, A., Ahmmed, S., Hossain, J., & Ismail, A. B. M. (2020). Solution-processed synthesisof copper oxide (Cu x O) thin films for efficient photocatalytic solar water splitting. *ACSomega*, *5*(39), 25125-25134. https://doi.org/10.1021/acsomega.0c02754

[3] Burgelman, M., Nollet, P. & Degrave, S. Modelling polycrystalline semiconductor solar cells. *Thin Solid Films* 361, 527-532 (2000).

[4] Chen, H., Ye, F., Tang, W., He, J., Yin, M., Wang, Y. & Han, L. (2017). A solvent-and vacuum-free route to large-area perovskite films for efficient solar modules. *Nature*, *550*(7674), 92-95.

[5] Cho, K. T., Paek, S., Grancini, G., Roldán-Carmona, C., Gao, P., Lee, Y., & Nazeeruddin, M.K.(2017). Highly efficient perovskite solar cells with a compositionally engineered perovskite/hole transporting material interface. *Energy & Environmental Science*, *10*(2), 621-627. https://doi.org/10.1039/C6EE03182J

[6] Danladi, E., Shuaibu, A., Ahmad, M. S., & Tasiu, J. (2021). Numerical modeling andanalysis of HTM-free heterojunction solar cell using SCAPS-1D. *East European Journal of Physics*, (2), 135-145. DOI:10.26565/2312-4334-2021-2-11

[7] Eli Danladi, Abdulazeez O. Salawu, Muhammed O. Abdulmalik, Emmanuel D Onoja, ElijahE. Onwoke and Damilare S. Adepehin . (2022). Optimization of Absorber and ETM Layer Thickness for Enhanced Tin based Perovskite Solar Cell Performance using SCAPS-1D Software, PHYSICS Access, Volume 02, Issue 01.https://doi.org/10.47514/phyaccess.2022.2.1.001

[8] Gao, P., Grätzel, M., & Nazeeruddin, M. K. (2014). Organohalide lead perovskites forphotovoltaic applications. *Energy & Environmental Science*, *7*(8), 2448-2463. https://doi.org/10.1039/C4EE00942H

[9] Haider, S. Z., Anwar, H., & Wang, M. (2018). A comprehensive device modelling of perovskite solar cell with inorganic copper iodide as hole transport material. *Semiconductor Science and Technology*, *33*(3), 035001. DOI 10.1088/1361-6641/aaa596

[10] Hossain, M. M., Jahan, N., & Hossain, R. U. (2022, February). Simulation and optimization of a highly efficient ZnO/Cu_2O/CdS/CdTe solar cell using SCAPS-1D. In *2022 International Conference on Advancement in Electrical and Electronic Engineering (ICAEEE)* (pp. 1-5).IEEE. https://doi.org/10.1109/ICAEEE54957.2022.9836410

[11] Islam, M. A., Jawad, A., Jahan, N. A., & Hossain, M. M. (2023). Outstanding conversion efficiency of 38.39% from a Perovskite/CIGS tandem PV cell: A synergic optimization through computational modeling. *Heliyon*, *9*(10).

[12] Jahan, N. A., Karim, M. M. U., & Hossain, M. M. (2018). A high efficiency ultra thin (1.8μm) CdS/CdTe pin solar cell with CdTe and Si as BSF layer. *Adv. Sci. Technol. Eng. Syst. J*, *3*(1), 213-217. https://dx.doi.org/10.25046/aj030125

[13] Jung, H. S., & Park, N. G. (2015). Perovskite solar cells: from materials to devices. *small*, *11*(1), 10-25. https://doi.org/10.1002/smll.201402767

[14] Karthicka, S., Velumania, S., Bouclé, J. (2020). Experimental and SCAPS simulatedformamidinium perovskite solar cells: Acomparison of device performance, Solar Energy205, 349–357.

[15]. Konstantakou, M., & Stergiopoulos, T. (2017). A critical review on tin halide perovskitesolar cells. *Journal of Materials Chemistry A*, *5*(23), 11518-11549. https://doi.org/10.1039/C7TA00929A

[16] Lim, K. G., Ahn, S., Kim, Y. H., Qi, Y., & Lee, T. W. (2016). Universal energy leveltailoring of self-organized hole extraction layers in organic solar cells and organic–inorganic hybrid perovskite solar cells. *Energy & Environmental Science*, *9*(3), 932-939. https://doi.org/10.1039/C5EE03560K

[17] Lim, K. G., Kim, H. B., Jeong, J., Kim, H., Kim, J. Y., & Lee, T. W. (2014). Boosting thepower conversion efficiency of perovskite solar cells using self-organized polymeric holeextraction layers with high work function. *Advanced materials*, *26*(37), 6461-6466.https://doi.org/10.1002/adma.201401775

[18] Memari, A., Javadian Sarraf, M., Seyyed Mahdavi Chabok, S. J., & Motevalizadeh, L. (2023). Comprehensive guidance for optimizing the colloidal quantum dot (CQD) Perovskite solar cells: experiment and simulation. *Scientific Reports*, *13*(1), 16675

[19] Muhammed, O. A., Danladi, E., Boduku, P. H., Tasiu, J., Ahmad, M. S. & Usman, N.(2021). Modeling and simulation of lead-free perovskite solar cell using SCAPS-1D. *East European Journal of Physics*, (2), 146-154. DOI:10.26565/2312-4334-2021-2-12

[20] NREL, Best research-cell efficiency chart. https://www.nrel.gov/pv/assets/pdfs/best-research-cell-efficiencies.pdf .

[21] Qazi, A., Hussain, F., Rahim, N. A., Hardaker, G., Alghazzawi, D., Shaban, K., & Haruna,K. (2019). Towards sustainable energy: a systematic review of renewable energy sources,technologies, and public opinions. *IEEE access*, *7*, 63837-63851.https://doi.org/10.1109/ACCESS.2019.2906402

[22] Rajamanickam, N., Kumari, S., Vendra, V. K., Lavery, B. W., Spurgeon, J., Druffel, T., &Sunkara, M. K. (2016). Stable and durable $CH_3NH_3PbI_3$ perovskite solar cells at ambientconditions. *Nanotechnology*, *27*(23), 235404. DOI 10.1088/0957-4484/27/23/235404

[23] Saga, T. (2010). Advances in crystalline silicon solar cell technology for industrial massproduction. *npg asia materials*, *2*(3), 96-102. doi: 10.1038/asiamat.2010.82

[24] Srivastava, S., Singh, A. K., Kumar, P., & Pradhan, B. (2022). Comparative performance analysis of lead-free perovskites solar cells by numerical simulation. *Journal of Applied Physics*, *131*(17). https://doi.org/10.1063/5.0088099

[25] Wang, D., Wright, M., Elumalai, N. K., & Uddin, A. (2016). Stability of perovskite solarcells. *Solar Energy Materials and Solar Cells*, *147*, 255-275.https://doi.org/10.1016/j.solmat.2015.12.025

[26] Wei, R. (2018). *Modelling of perovskite solar cells* (Doctoral dissertation, Queensland University of Technology). https://doi.org/10.5204/thesis.eprints.119218

[27] Yang, W. S., Park, B. W., Jung, E. H., Jeon, N. J., Kim, Y. C., Lee, D. U. & Seok, S. I.(2017). Iodide management in formamidinium-lead-halide–based perovskite layers for efficient solar cells. *Science*, *356*(6345), 1376-1379. https://doi.org/10.1126/science.aan2301